

The feasible constant speed helical trajectories for propeller driven airplanes

Gilles Labonté*

*Department of Mathematics and Computer Science, Royal Military College of Canada,
Kingston, Ontario, Canada*

(Received November 1, 2016, Revised February 11, 2016, Accepted February 13, 2016)

Abstract. The motion of propeller driven airplanes, flying at constant speed on ascending or descending helical trajectories is analyzed. The dynamical abilities of the airplane are shown to result in restrictions on the ranges of the geometrical parameters of the helical path. The physical quantities taken into account are the variation of air density with altitude, the airplane mass change due to fuel consumption, its load factor, its lift coefficient, and the thrust its engine can produce. Formulas are provided for determining all the airplane dynamical parameters on the trajectory. A procedure is proposed for the construction of tables from which the flyability of trajectories at a given angle of inclination and radius can be read, with the corresponding minimum and maximum speeds allowed, the final altitude reached and the amount of fuel burned. Sample calculations are shown for the Cessna 182, a Silver Fox like unmanned aerial vehicle, and the C-130 Hercules.

Keywords: airplane helical trajectory; banked turn; airplane equation of motion; circular arc connection; automatic trajectory planning

1. Introduction

This work constitutes a contribution to the enterprise of endowing unmanned aerial vehicles (UAVs) with complete autonomy, i.e., the ability to conduct their mission without human intervention. A fundamental task they then have to be able to perform consists in automatically re-planning their trajectory when unforeseen circumstances require them to modify their flight plan. Essential tools to perform this task are formulas or tables which indicate what trajectories are flyable, according to the airplane dynamics, and provide basic information such as the amount of fuel required, the time of flight, etc.

It is important to remark that for producing optimal or very good trajectories, many factors have to be analyzed, not only properties of the mathematical curve itself but very much also those of the vehicle involved. Whereas the authors of the first studies on trajectory planning in 3D were mainly interested in finding the shortest curve between two points with departure and arrival directions (for example Dubins (1957)), present studies now define optimality by taking into account many more factors than the length. Firstly, of course, the vehicle considered should have

*Corresponding author, Emeritus Professor, E-mail: gilles.labonte@rmc.ca

the physical ability to travel the curve in question. Finding the optimal trajectory then becomes a multi-objective optimization problem. A cost function is usually defined that takes into account the relative importance of the amount of fuel used, of the travel time, of the altitude. The relative importance of each factor has to be weighed according to the mission flown. Thus, finding optimal airplane trajectories involves analyzing the mathematical curves, the aerodynamic abilities of the airplane, and other factors that depend on the nature of the terrain.

Frazzoli *et al.* (2005) have introduced an efficient approach for the solution of the trajectory planning problem. Namely, they proposed to construct trajectories by concatenating well-defined motion primitives, i.e., elementary trajectory segments, selected from a finite library. All the required properties of these elementary segments could be computed offline if necessary, and stored in the memory of the airplane controller. The appeal of this approach resides in that it would save much computing efforts because only the connections between the pieces of trajectory would have to be computed on-board. As far as airplanes are concerned, the most often considered elementary segments are rectilinear, circular and helical.

A relatively similar technique for building feasible trajectories proceeds as follows. One starts by building a skeleton trajectory with connected rectilinear segments, and then smooths out the connections with arcs of circles so that the velocity can be continuous. This very popular method can be found described, for example, in Chandler *et al.* (2000), Jia and Vagners (2004), Chitsaz and LaValle (2007), Hwangbo *et al.* (2007), Li Xia *et al.* (2009), Ambrosino *et al.* (2009), Babaei and Mortazavi (2010), Hota and Ghose (2010). We note that, although such constructions, which use only straight lines and circles, are often sufficient to produce flyable trajectories, this method is incomplete because there are situations in which the transition to higher or lower altitudes could only be done with the help of helical trajectory segments, due of the narrowness of the space available for the motion. Furthermore, as demonstrated in Sussmann (1995), there are situations in which the inclusion of helical segments is necessary for obtaining the shortest path, which the optimal trajectory is often required to be.

An approach, in which helical trajectories are included as elementary sub-trajectories should then be preferred. This was in fact used by many researchers such as Boukraa *et al.* (2006), Chitsaz and LaValle (2007), Narayan *et al.* (2008), Tsiotras *et al.* (2011) and Beard and McLain (2015). The helices usually considered are of the same type as those we analyze in the present study; that is, they are regular pitch curves wrapping around a cylinder with center along the vertical axis. There are however more general helices as defined for example in Sussmann (1995). We note that the vertical regular helices cannot start and end at arbitrary points with arbitrary direction of departure and approach. They can have arbitrary initial conditions, but these conditions leave no additional choice in selecting the helix parameters. Thus, if a final position is specified, the final direction of approach is uniquely determined. Therefore, an additional segment of curve, as an arc of circle, is necessary to connect the helix to the end point with the desired direction of approach, or the next segment of curve.

Helical trajectories have also been considered in their own right. Crawford and Bowles (1975) argued that it may be advantageous for an airplane to follow a helical trajectory when landing in a densely populated district, from the standpoint of safety and noise. Indeed, such a flight path keeps the airplane at relatively high altitude except near the airport. Similarly, Tsiotras *et al.* (2011) presented a method for finding the time-optimal landing trajectory of an airplane that involved helical trajectories. Dai and Cochran (2009) considered the helical trajectory as starting point for constructing minimum-time-to-climb and minimum-fuel-to-climb trajectories for an airplane constrained in a vertical rectangular prism region.

Most studies on airplane trajectory planning adopt the airplane model described by Dubins (1957), according to which the airplane flies at constant speed, while it is constrained by bounds on the vertical component of its velocity and its turning radius. More sophisticated airplane models have also been used, which include to various degrees, more realistic airplane dynamics. In the present study, we have considered the realistic airplane dynamics model described in Anderson (2000).

The motion of airplanes on straight line segments and circular segments has been analyzed in details in Labonté (2012), (2015), (2016). However, a corresponding analysis of helical trajectory has still not been done. Although banked turns or coordinated turns in the horizontal plane are discussed in most aeronautics manuals, only a few of them mention the case of bank turns accompanied by vertical motion. This can be found, for example, in Section 15 of Colwley and Levy (1920), in Section 10.4 of Etkin (1972), in Section 8.2 of Mair and Birdsall (1992) and in Chapter 3 of Phillips (2004). In all these discussions of helical trajectories, the speed and the vertical component of the velocity are considered constant. All the above mentioned authors, except for Colwley and Levy (1920), consider small elevation angles θ_H with respect to the horizontal, so that $\sin(\theta_H) \approx \theta_H$ and $\cos(\theta_H) \approx 1$. However, UAVs come in a wide range of sizes and agilities, and they can fly much more daring maneuvers as inhabited airplanes. This is also the case for high performance fighter airplanes. There are therefore many circumstances in which the small elevation angle approximation is not justified. We note that many of the discussions involving helical trajectories use equations of motion, similar to those we used in our study. However, very rarely do they take into account the variation of the airplane dynamical parameters with altitude, as the air density varies, and only Dai and Cochran (2009) consider the amount of fuel used. The present study is more complete in that it determines the limits on the trajectory parameters that are a consequence of the limits on the airplane load factor, its lift coefficient, its available power, while taking into account the influence of altitude. It also presents a formula for calculating the amount of fuel required to fly on the helical trajectory.

1.1 Assumptions about the dynamics

As was pointed out in Section 15 of Cowley and Levy (1920), a rigorous treatment of curved flight trajectories is extremely complicated because of the presence of imperfectly known factors related to the variation in aerodynamic forces along the wings, due to their non-symmetric role in the motion. These authors then assumed that “any increase of drag due to the angular velocity of the aircraft and the deflections of the control surfaces can be neglected in comparison with the dominant lift-dependent drag”. This was actually confirmed in Chapter XVIII of Von Mises (1945) where, after some calculations, for the banked turn, the comment is made that, “the moments required for maintaining the steady rotation are unimportant under normal conditions”. A similar remark can be found in Section 8.5 of Chapter 8 of Mair and Birdsall (1992), in the context of a detailed discussion of vertical loops, horizontal banked turns and helical trajectories.

In the present study, we have made the same assumption that the effects of the rotations of the airplane about its center of mass are negligible compared to those of the motion of its center of mass. We have also not taken into account the perturbations of the atmosphere. Finally, we make our remark made in Chapter 3 on “Aircraft Performance” of Phillips (2004), that the material we present “should be thought of as only a preliminary study of airplane performance. Here, emphasis is placed on obtaining closed-form analytic solutions suitable for preliminary design”.

1.2 Power available, power required and fuel consumption

As explained in Chapter 9 of Anderson (2000), when an internal combustion engine produces the power P_p to activate a propeller of efficiency η , the power available to move the airplane is $P_A = \eta(J)P_p$. The efficiency of the propeller η is a function of the advance ratio J , defined as

$$J = \frac{V_\infty}{ND}$$

in which N is its number of revolution per second and D is its diameter. If P_{\max} is the maximum power that the engine can produce, the maximum power available $P_{A\max}$ to move the airplane is

$$P_{A\max} = \eta(J)P_{\max}$$

If W represents the weight of the airplane, and c the specific fuel consumption, then the rate of fuel burned for producing the power P_A is

$$\frac{dW}{dt} = -c P_p = -\frac{c}{\eta} P_A$$

There is always an upper bound $P_{A\max}$ to the power an engine can generate and a lower bound $P_{A\min}$ below which it shuts down.

According to Classical Mechanics, the power required P_R to move a body with velocity \mathbf{v} , is $P_R = \mathbf{F} \cdot \mathbf{v}$, where \mathbf{F} is the force acting on the body and “ \cdot ” denotes the scalar product of two vectors. If this body is an airplane with a propulsion system that produces a thrust \mathbf{T} along the direction of its motion, i.e., \mathbf{T} is parallel to \mathbf{v} , then the power required for the motion is $P_R = T V$ where T and V are respectively the magnitudes of \mathbf{T} and \mathbf{v} . This airplane’s engine should then provide the power $P_A = P_R$. It is important to note that the power produced by a combustion engine varies with the altitude h , according to the equation

$$P_A(h) = P_A(0) \frac{\rho(h)}{\rho(0)}$$

in which $\rho(h)$ is the air density at altitude h .

1.3 Organisation of the article

The first section explains the mathematical description of the motion of an airplane on a helical trajectory, while its speed of rotation about the vertical axis and the vertical component of its velocity are constant. This description takes into account the weight change of the airplane as fuel is burned, and the variation of some parameters with the altitude. The equations of motion are then decomposed in terms of the Frenet-Serret unit vectors. The consequences of the bounds on the angle of bank, the load factor, the lift coefficient are analyzed. The formula that gives the weight of the airplane, as a function of time is given. The thrust required for the motion is examined. The consequences for a descending trajectory of the non-negativity of the thrust are obtained. The constraints on trajectories that result from the upper boundedness of the power available are derived. Finally, a procedure is proposed to take into account the limits imposed on the trajectory by the airplane dynamics, and determine the parameters for which this trajectory is flyable. It is shown how tables of parameters can be constructed to sum up the results obtained. This procedure

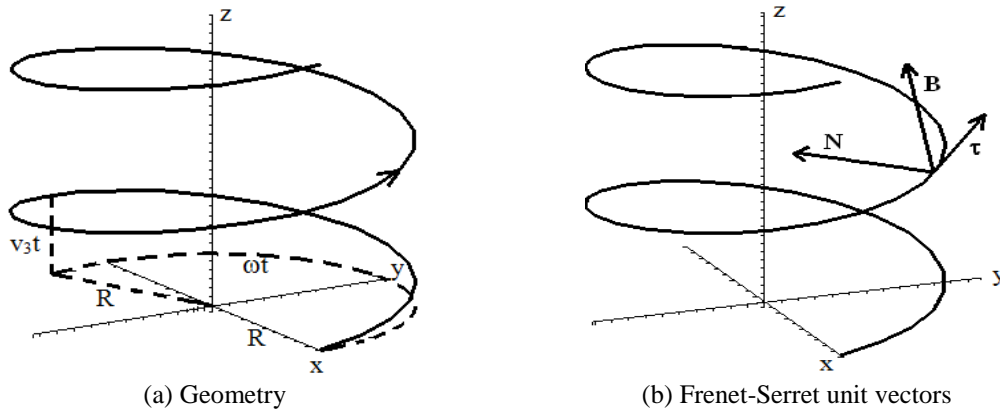


Fig. 1 Ascending helical trajectory

is illustrated, for both cases of ascending and descending trajectories, with airplanes that have similar properties as the following well known three different airplanes, the required characteristics of which are listed in Appendix A:

- the Cessna 182 Skylane, which has a constant speed propeller,
- a Silver Fox like unmanned aerial vehicle (UAV) which has a fixed pitch propeller,
- the C-130 Hercules, which has a constant speed propeller.

2. Description of constant speed helical trajectories

Let us consider an airplane that flies on a vertical axis helical trajectory at the constant speed V_∞ , with constant vertical speed v_3 . We select the coordinate system such that the helix is centered on the z-axis, and passes through the point $(R, 0, 0)$ at $t=0$. The position of the center of mass of the airplane is then described by

$$\mathbf{x}(t) = [R \cos(\omega t), \varepsilon R \sin(\omega t), v_3 t]$$

in which $\varepsilon=+1$ if the trajectory turns about the z-axis in the counterclockwise direction and $\varepsilon=-1$ if it turns in the other direction. R and ω are respectively the constant radius and the constant frequency of rotation of the circular section of the trajectory. Fig. 1(a) shows such a trajectory with $\varepsilon=+1$, and $v_3>0$. When the airplane is descending on the trajectory, v_3 will be negative.

The velocity on this trajectory is

$$\mathbf{v}(t) = [-R\omega \sin(\omega t), \varepsilon R\omega \cos(\omega t), v_3]$$

and the constant speed V_∞ is,

$$V_\infty = \sqrt{R^2 \omega^2 + v_3^2}$$

If θ is the angle of ascension of the helix, measured from an horizontal plane, then $0 \leq |\theta| < \pi/2$ and $v_3 = V_\infty \sin(\theta)$ and $R\omega = V_\infty \cos(\theta)$. θ is positive when the airplane is ascending and negative when it is descending. The Frenet-Serret frame of reference $\{\tau, \mathbf{N}, \mathbf{B}\}$ is particularly useful in the description of such trajectories. Fig. 1(b)

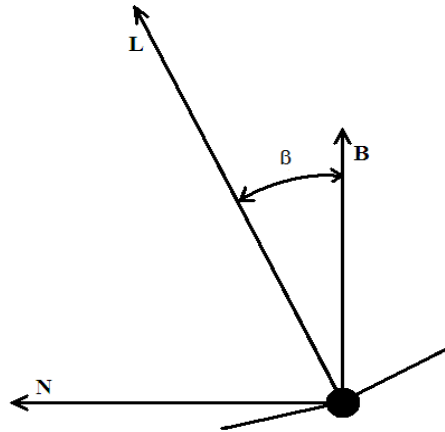


Fig. 2 The angle of bank in relation to the unit vectors \mathbf{N} and \mathbf{B}

shows the three unit vectors, $\boldsymbol{\tau}$, \mathbf{N} and \mathbf{B} with respect to the helix shown in Fig. 1(a). $\boldsymbol{\tau}$ is the unit tangent vector that is in the direction of the velocity

$$\boldsymbol{\tau} = [-\cos(\theta)\sin(\omega t), \varepsilon\cos(\theta)\cos(\omega t), \sin(\theta)]$$

Since $\frac{ds}{dt} = V_\infty$, the arc length s , that is the distance traveled between times t_s and t_f is simply

$$s = V_\infty (t_f - t_s).$$

The difference of altitude between these two instants of time is

$$\Delta h = v_3(t_f - t_s)$$

The unit normal vector \mathbf{N} is defined such that

$$\frac{d\boldsymbol{\tau}}{ds} = \kappa\mathbf{N} \quad \text{with} \quad \kappa = \frac{1}{R_c}$$

in which κ is the curvature and R_c is the radius of curvature. Thus

$$R_c = \frac{R}{\cos^2 \theta} \quad \text{and} \quad \mathbf{N} = -[\cos(\omega t), \varepsilon\sin(\omega t), 0]$$

The acceleration of the airplane on this trajectory is

$$\mathbf{a}(t) = \mathbf{v}'(t) = \frac{V_\infty^2}{R_c} \mathbf{N}(t)$$

The unit binormal vector \mathbf{B} , which is defined as $\boldsymbol{\tau} \times \mathbf{N}$, is

$$\mathbf{B} = [\varepsilon \sin(\theta) \sin(\omega t), -\sin(\theta) \cos(\omega t), \varepsilon \cos(\theta)].$$

Note that for a trajectory that rotates in the clockwise direction with respect to the z -axis, \mathbf{B} is pointing downward.

3. The forces at play

The physical forces at play are

- the lift \mathbf{L} ,
- the gravitational force $\mathbf{W} = -W\mathbf{k}$, with $\mathbf{k} = (0, 0, 1)$,
- the longitudinal force that is composed of the thrust produced by the propulsion system T , and the drag D ; its value is $(T-D)\boldsymbol{\tau}$.

The lift \mathbf{L} is perpendicular to the velocity of the airplane and the airplane bank angle, is measured with respect to the binormal of the trajectory. Thus, \mathbf{L} can be written as

$$\mathbf{L} = L \cos(\beta) \mathbf{B}(t) + L \sin(\beta) \mathbf{N}(t)$$

Fig. 2 shows the bank angle relative to the Frenet-Serret unit vectors.

The mass of the airplane changes as fuel is burned by its engines. It increases as the motors intake air that is at rest, in order to burn its fuel, and it decreases as the hot gases of combustion are ejected with a speed essentially equal to the airplane speed. The mass of air M_{air} required for combustion is proportional to the mass of fuel burned M_{fuel} , as $M_{\text{air}} = \text{AFR} \cdot M_{\text{fuel}}$, in which ‘‘AFR’’ denotes the air to fuel ratio, which is about 14.7 for gasoline or diesel fuel (Kamm 2002). Labonté (2012) discussed how to allow for these processes in Newton’s equation of motion, and showed that the proper form to use for that equation is then

$$\frac{W}{g} \mathbf{a} - \frac{(\text{AFR})}{g} \left[\frac{dW}{dt} \right] \mathbf{v} = \mathbf{L} + \mathbf{W} + (T - D) \boldsymbol{\tau} \quad (1)$$

The \mathbf{B} , \mathbf{N} and $\boldsymbol{\tau}$ components of this equation are respectively

$$L \cos(\beta) = W \varepsilon \cos(\theta) \quad (2)$$

$$L \sin(\beta) = W A_c \quad \text{with} \quad A_c = \frac{V_\infty^2}{g R_c}, \quad (3)$$

$$T = D + W \sin(\theta) - \frac{(\text{AFR}) V_\infty}{g} \left(\frac{dW}{dt} \right) \quad (4)$$

the variable A_c has been defined as the centripetal acceleration in units of g .

4. The bank angle

Upon dividing Eq. (3) by Eq. (2), the following equation is obtained for the bank angle

$$\tan(\beta) = \frac{\varepsilon A_c}{\cos(\theta)}$$

This equation indicates that all airplanes must bank with the same angle in order to travel with the same speed V_∞ on this helical trajectory, a fact that generalises a well-known property of horizontal circular trajectories. Furthermore, the bank angle is constant on the whole trajectory. Given the signs of $\sin(\beta)$ and $\cos(\beta)$, according to Eqs. (2) and (3), if the trajectory is counter-

clockwise, $\varepsilon=+1$ and $0 < \beta < \pi/2$; and if it is clockwise $\varepsilon=-1$ and $\pi/2 < \beta < \pi$. Thus

$$\sin(\beta) = \frac{A_c}{\sqrt{\cos^2(\theta) + A_c^2}} \quad \cos(\beta) = \frac{\varepsilon \cos(\theta)}{\sqrt{\cos^2(\theta) + A_c^2}} \quad (5)$$

5. The load factor

According to Eq. (2), the load factor is

$$n = \frac{L}{W} = \sqrt{\cos^2(\theta) + A_c^2} \quad (6)$$

It is constant on the trajectory. In order to ensure the integrity of the airplane structure, its value has to be limited such that

$$n_{min} \leq n \leq n_{max}$$

Since n is always non-negative, this inequality implies that

$$V_\infty \leq V_{UBI} \quad V_{UBI} = \frac{\sqrt{gR} [n_{max}^2 - \cos^2(\theta)]^{1/4}}{\cos(\theta)} \quad (7)$$

For a Cessna 182, on an helix with $\theta=15^\circ$, and $R=750$ m, this inequality implies that $V_\infty \leq 170.2$ m/s.

6. The lift coefficient

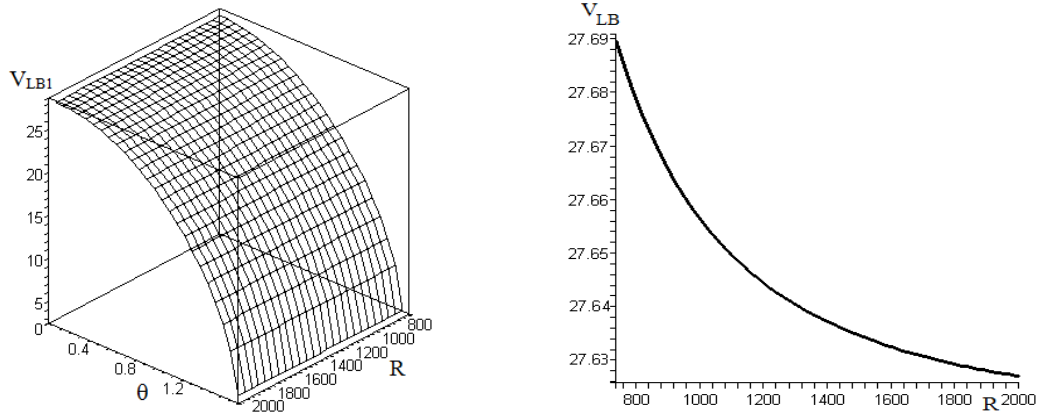
Upon replacing L by its expression in Eq. (6), the following expression for the lift coefficient C_L can be derived

$$C_L = \frac{2W}{\rho_\infty S V_\infty^2} \sqrt{\cos^2(\theta) + A_c^2} \quad (8)$$

C_L changes in time because W and ρ_∞ do. It must satisfy the constraint $C_L \leq C_{Lmax}$. This constraint on C_L is respected if and only if it is respected at the instant at which C_L has its maximum value, which is at the time at which W/ρ_∞ is maximum. For descending flights, W/ρ_∞ is a monotonically decreasing function of time since W is monotonically decreasing while ρ_∞ is monotonically increasing. Thus, W/ρ_∞ is maximum at the beginning of the descent, when $t=t_i$. The constraint $C_L \leq C_{Lmax}$ is then satisfied if and only if

$$\frac{2W_i}{\rho_\infty(h_i) S V_\infty^2} \sqrt{\cos^2(\theta) + A_c^2} \leq C_{Lmax} \quad (9)$$

in which $W_i=W(t_i)$ and h_i is the initial altitude. For ascending flights, the time at which the maximum of C_L occurs is less evident because then, both W and ρ_∞ are monotonically decreasing with time. Determining where the maximum of C_L occurs would require solving for $W(t)$, but solving for W requires knowing the trajectory parameters, which satisfy the bound $C_L \leq C_{Lmax}$.



(a) Lower bound surface for \$V_\infty\$ (\$\theta\$ in radians) (b) Lower bound line for \$V_\infty\$ at \$\theta=15^\circ\$
 Fig. 3 Bound on the speed \$V_\infty\$ due to the bound on the lift coefficient for the Cessna 182

Nevertheless, a sufficient condition can be derived by using the absolute upper bound on \$W/\rho_\infty\$ in Ineq. (8). Indeed, if Ineq. (8) is satisfied with \$W_i/\rho_\infty(h_c)\$, where \$h_c\$ is the service ceiling of the airplane, it will necessarily be satisfied with any value of \$W/\rho_\infty\$. Upon substituting the value of \$A_c\$ in Ineq. (9) and rearranging the terms, this necessary condition can be written as

$$\left[\left(\frac{(C_{L,max} \rho_\infty(h_x) S)}{2W_i} \right)^2 - \left(\frac{\cos^2(\theta)}{gR} \right)^2 \right] V_\infty^4 \geq \cos^2(\theta) \tag{10}$$

in which \$h_x=h_i\$ or \$h_c\$ according to whether the trajectory is descending or ascending. This inequality can hold only if the first factor on the LHS is positive, which requires the following condition on \$R\$

$$R > \frac{2W_i \cos^2(\theta)}{\rho_\infty(h_x) S C_{L,max}} \tag{11}$$

Ineq. (10) then implies the following inequality for \$V_\infty\$

$$V_\infty \geq V_{LB1} \text{ with } V_{LB1}(R, \theta) = \frac{[2gRW_i \cos(\theta)]^{1/2}}{\left[(gR\rho_\infty(h_x) S C_{L,max})^2 - (2W_i \cos^2(\theta))^2 \right]^{1/4}} \tag{12}$$

For the Cessna 182, the speeds \$V_\infty\$ for which Ineq. (12) holds are those in the region above the surface, shown in Fig. 2(a). Fig. 3(b) shows the slice of this graph, at \$15^\circ\$. One can see from these graphs that the lower bound on \$V_\infty\$ does not vary much with \$R\$; in Fig. 3(b), the speed varies approximately between 27.62 and 27.69 m/s, as \$R\$ varies from 800 to 2000 m. On a helix with \$\theta=15^\circ\$, and \$R=750\$ m, Ineq. (12) implies that \$V_\infty \ge 27.7\$ m/s.

7. The airplane weight

For the sake of clarity, we shall hereafter consider counter-clockwise turning trajectories so that \$\epsilon=+1\$; the case with \$\epsilon=-1\$ can be dealt with in the same way. Since the power required for the

motion is $P_R = V_\infty T_R$, we multiply Eq. (4) by $-\frac{c}{\eta} V_\infty$ and use Eq. (10) to obtain the following equation for the weight of the airplane

$$\left[1 - \frac{c(\text{AFR})V_\infty^2}{\eta g} \right] \left[\frac{dW}{dt} \right] = -\frac{cV_\infty}{\eta} [D + W \sin(\theta)] \quad (13)$$

We will consider here flights below 11 km, so that the rate of variation of the temperature with the altitude a_1 is constant, and

$$T(h) = T_s - a_1 h \text{ with } a_1 = 6.5 \times 10^{-3} \text{ K/m.}$$

In a flight at a constant speed, the rate of climb is constant and the altitude is simply a linear function of time

$$h(t) = h_i + v_3 (t - t_i) \text{ with } v_3 = V_\infty \sin(\theta).$$

So the time to change altitude from h_i to h_f is simply $t_f = (h_f - h_i) / v_3$. The results we shall obtain can be straightforwardly extended to airplanes traversing zones of the atmosphere with different temperature gradients by interconnecting the solutions obtained in the separate zones, so that the parameters are continuous at the boundary layers between the zones.

Upon letting $W_f = W(t_f)$ and upon using Eq. (8), Eq. (13) becomes the Riccati equation

$$\frac{dW}{dt} = -\left[\alpha T^{4.2433} + \beta W + \delta T^{-4.2433} W^2 \right] \quad (14)$$

in which α , β and δ are the following constants

$$\alpha = \alpha_1 \frac{V_\infty^3}{G}, \quad \beta = \beta_1 \frac{V_\infty}{G}, \quad \delta = \delta_1 \frac{1}{V_\infty G} + \delta_2 \frac{V_\infty^3}{G} \quad \text{with} \quad (15)$$

$$\alpha_1 = \frac{c g \rho_s S C_{D0}}{2 T_s^{4.2433}}, \quad \beta_1 = c g \sin(\theta), \quad \delta_1 = \frac{2 c g T_s^{4.2433} \cos^2(\theta)}{\pi e A R \rho_s S}, \quad \delta_2 = \frac{\delta_1 \cos^2(\theta)}{g^2 R^2},$$

$$G(V_\infty) = \left[\eta (V_\infty) g - c(\text{AFR}) V_\infty^2 \right].$$

We have written the constants, in such a way as to factor out their dependence on V_∞ , as this will prove useful in our analysis. For the three representative airplanes considered as examples, $G(V_\infty)$ is positive for all V_∞ ; this is expected to be the case for all airplanes.

We remark that Eq. (14) is the same one as obtained in Labonté (2012) for an airplane that moves at constant speed on an inclined rectilinear trajectory with the inclination angle θ . The only difference resides in the parameter δ , which contains here the additional radial acceleration term A_c^2 . The solution of Eq. (14) is therefore the same combination of confluent hypergeometric functions as described in Labonté (2012). Labonté (2015) has showed that a one-step Runge-Kutta approximation of order four produces essentially the exact value of $W(t)$. This is this solution that we shall use hereafter.

7.1 Calculating the weight

According to the one-step Runge-Kutta approximation of order four, the weight of the airplane is given by $W(t)$

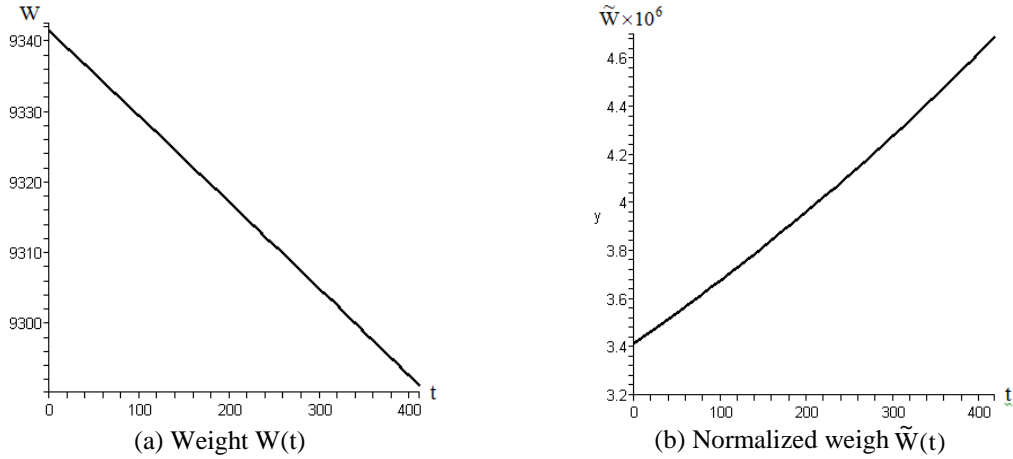


Fig. 4 Weight variation in time for a Cessna 182 ascending on a helix with $\theta=15^0$, $R=750$ m and $V_\infty=30$ m/s

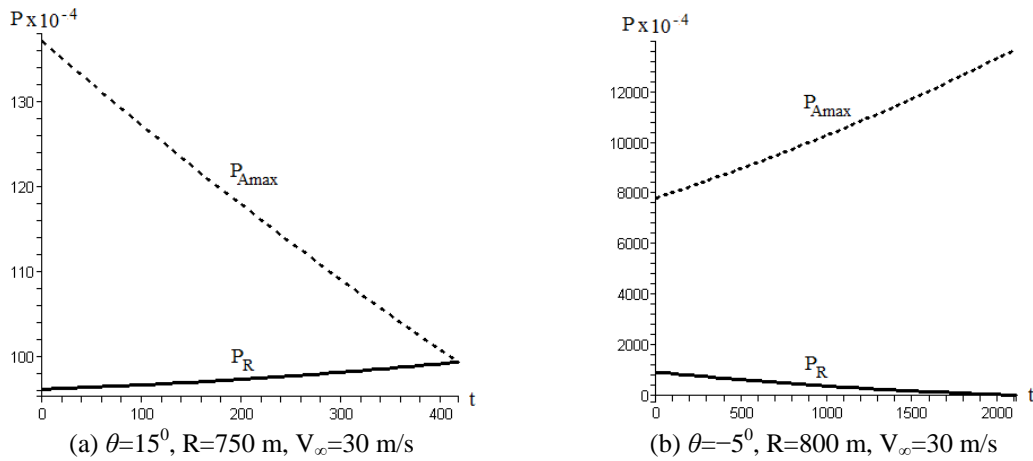


Fig. 5 Power required P_R (solid line) and the maximum power available P_{Amax} (dotted line), for the Cessna 182

$$W(t) = W_i + \frac{1}{6} [A(t) + 2B(t) + 2C(t) + D(t)]$$

in which $A(t)=t F(t_i, W_i)$, $B(t)=t F(t_m, W_i+A(t)/2)$, $C(t)=t F(t_m, W_i+B(t)/2)$, $D(t)=t F(t_m, W_i+C(t))$

$$F(t, W) = -\left\{ \alpha T[h(t)]^{4.2433} + \beta W + \delta T[h(t)]^{-4.2433} W^2 \right\} \text{ and } \Delta t = t - t_i, \quad t_m = t_i + \Delta t/2. \quad (16)$$

Fig. 4(a) shows how W varies with time, as the Cessna 182, ascends on a helical trajectory inclined at 15^0 , with radius $R=750$ m and speed $V_\infty=30$ m/s, to the maximum altitude it can attain. One can see that for such a trajectory, W is essentially a linear function of time; thus the linear approximation for $W(t)$, discussed in Labonté (2015) could very well be used. We shall hereafter use the variable $\tilde{W} = W/T(h)^{4.2433}$; Fig. 4(b) shows how \tilde{W} varies with time, for the same trajectory as in Fig. 4(a).

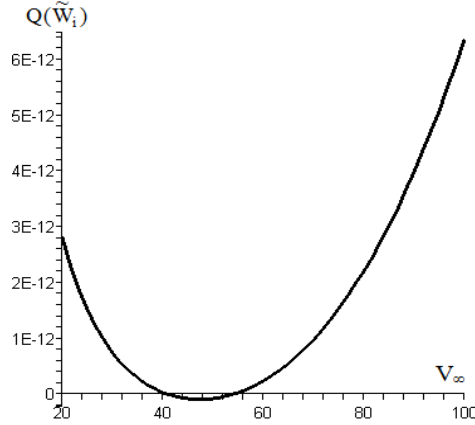


Fig. 6 $Q(\tilde{W}_i)$ as a function of V_∞ for the Cessna 182, when $\theta=-5^\circ$ and $R=800$ m

8. The power required

Eq. (1) states that

$$P_R = \frac{\eta}{c} \left[\alpha T^{4.2433} + \beta W + \delta T^{-4.2433} W^2 \right] \quad (17)$$

Fig. 5(a) shows how the power required P_R and the power available P_{Amax} vary with time, as the Cessna 182, ascends on a helical trajectory with $R=750$ m, $\theta=15^\circ$ to the maximum altitude $h_f=3246$ m, that it reaches at $t_f=418$ s. After this altitude the power required to ascend is greater than the maximum power available P_{Amax} from its engine-propeller system. Fig. 5(b) shows how P_R and P_{Amax} vary when the Cessna 182 is descending with $\theta=-5^\circ$, $R=800$ m and $V_\infty=30$ m/s.

8.1 Non-negativity of the power required

The power required for the motion of the airplane P_R should obviously be non-negative. When the airplane is not descending, the constants α and δ are positive and β is non-negative. Thus the right-hand side (RHS) of Eq. (14) is negative and the weight of the airplane is decreasing. Thus, according to the RHS of Eq. (17), the power required is positive. However, when the airplane is descending, β is negative so that some conditions are required to ensure that $P_R \geq 0$. P_R can then be written as

$$P_R = \frac{\eta}{c} T^{4.2433} Q(\tilde{W}) \quad \text{with } Q(\tilde{W}) = \alpha + \beta \tilde{W} + \delta \tilde{W}^2 \quad (18)$$

Since P_R , and thus Q , must be non-negative for all values of \tilde{W} on the trajectory, this must definitely be the case for its initial value \tilde{W}_i . Upon replacing, α , β and δ by their value, given in Eq. (15), this necessary condition $Q(\tilde{W}_i) \geq 0$ can be written as

$$\left(\alpha_1 + \delta_2 \tilde{W}_i^2 \right) V_\infty^4 + \left(\beta_1 \tilde{W}_i \right) V_\infty^2 + \left(\delta_1 \tilde{W}_i^2 \right) \geq 0 \quad (19)$$

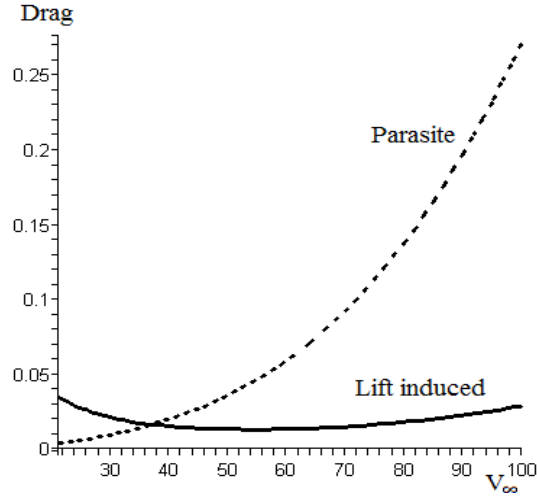


Fig. 7 Lift induced drag (full line) and parasite drag (dotted line) for the Cessna 182

Fig. 6 shows how $Q(\tilde{W}_i)$ varies in term of the speed V_∞ for the Cessna 182, when $\theta=-5^\circ$ and $R=800$ m. The left-hand side (LHS) of Ineq. (19) is a quadratic expression in V_∞^2 . Its discriminant Δ_0 is

$$\Delta_0 = \beta_1^2 \tilde{W}_i^2 - 4(\alpha_1 + \delta_2 \tilde{W}_i^2) \delta_1 \tilde{W}_i^2 \tag{20}$$

If the parameters R and θ are such that $\Delta_0 < 0$, then the expression on the LHS of Ineq. (19) does not have real roots, and therefore Ineq. (19) is satisfied for all V_∞ . If they are otherwise such that $\Delta_0 > 0$, then the LHS of Ineq. (19) has two positive real roots r_{0-} and r_{0+}

$$r_{0\pm} = \frac{1}{2(\alpha_1 + \delta_2 \tilde{W}_i^2)} \left[-\beta_1 \tilde{W}_i \pm \sqrt{\Delta_0} \right] \tag{21}$$

and the LHS of Ineq. (19) is non-negative for all V_∞ except those in the forbidden interval $\bar{I}_V = (\sqrt{r_{0-}}, \sqrt{r_{0+}})$ where $Q(\tilde{W}_i) < 0$. For the flight shown in Fig. 6, $\bar{I}_V = (41.0, 53.9)$ m/s.

As can be seen in Eqs. (5)-(7), the lift cancels the component of gravity that is perpendicular to the velocity, and the drag cancels its component along the velocity. Thus, the drag must be strong enough to cancel this effect of the force of gravity for the speed to remain constant. It is interesting to note that the two separate domains $V_\infty \leq \sqrt{r_{0-}}$ and $V_\infty \geq \sqrt{r_{0+}}$ correspond respectively to the regions in which it is the lift induced drag and the parasite drag that dominates the force of gravity. In Fig. 7 the full line and the dotted line represent respectively the lift induced drag and the parasite drag. These forces dominate respectively at low and large speeds. However, this ceases to be the case in the interval \bar{I}_V , in which the airplane would therefore accelerate.

Once it has been ensured, by selecting a speed outside of \bar{I}_V , that P_R is non-negative at the initial time $t=t_i$, some conditions must still be imposed for it to remain non-negative at all later times. In order to find these conditions, we shall examine the properties of Q , considered as a second degree polynomial in \tilde{W} . It corresponds to a convex parabola, with minimum at

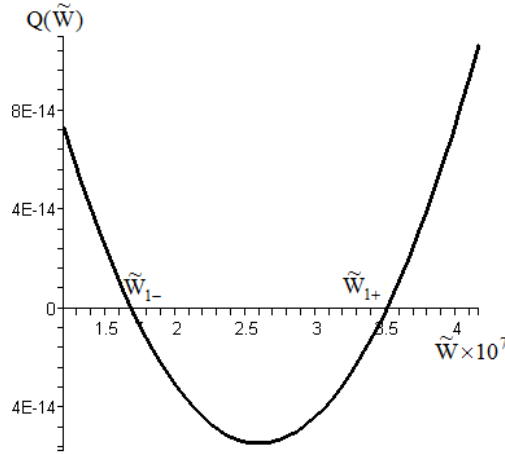


Fig. 8 $Q(\tilde{W})$ in terms of \tilde{W} , for the Cessna 182, with $V_\infty=30$ m/s, $\theta=-5^\circ$ and $R=800$ m

$\tilde{W} = -\frac{\beta}{2\delta}$ and positive intercept on the ordinate axis. This parabola does not change in time. The discriminant of Q is $\Delta_1 = \beta^2 - 4\alpha\delta$, and two cases should be distinguished according to the sign of Δ_1 .

Case 1: $\Delta_1 < 0$

Then $Q(\tilde{W})$ does not have real roots and it is positive for all \tilde{W} , without additional conditions being required.

Case 2: $\Delta_1 \geq 0$

$Q(\tilde{W})$ has two positive real roots \tilde{W}_{1-} and \tilde{W}_{1+}

$$\tilde{W}_{1\pm} = \frac{1}{2\delta} \left[-\beta \pm \sqrt{\Delta_1} \right] \tag{22}$$

which do not change with time. $Q(\tilde{W})$ is non-negative everywhere except when \tilde{W} is in the interval $\tilde{I}_{\tilde{W}} = (\tilde{W}_{1-}, \tilde{W}_{1+})$. Fig. 8 shows how $Q(\tilde{W})$ varies with \tilde{W} for the Cessna 182, with $V_\infty=30$ m/s, $\theta=-5^\circ$ and $R=800$ m.

Consequently, we shall distinguish two sub-cases, which correspond to the position of \tilde{W}_i relative to this interval.

Case 2a: $\tilde{W}_i \leq \tilde{W}_{1-}$

Since P_R is non-negative at \tilde{W}_i , it will remain non-negative for all times after t_i since $\tilde{W}(t)$ is a monotonically decreasing function of t .

Case 2b: $\tilde{W}_i \geq \tilde{W}_{1+}$

P_R is then non-negative at \tilde{W}_i . The value of P_R then decreases as $\tilde{W}(t)$ decreases. This would be the situation for the trajectory shown in Fig. 8.1, for which $\tilde{W}_i = 6 \times 10^{-7}$. Thus, in order for P_R to

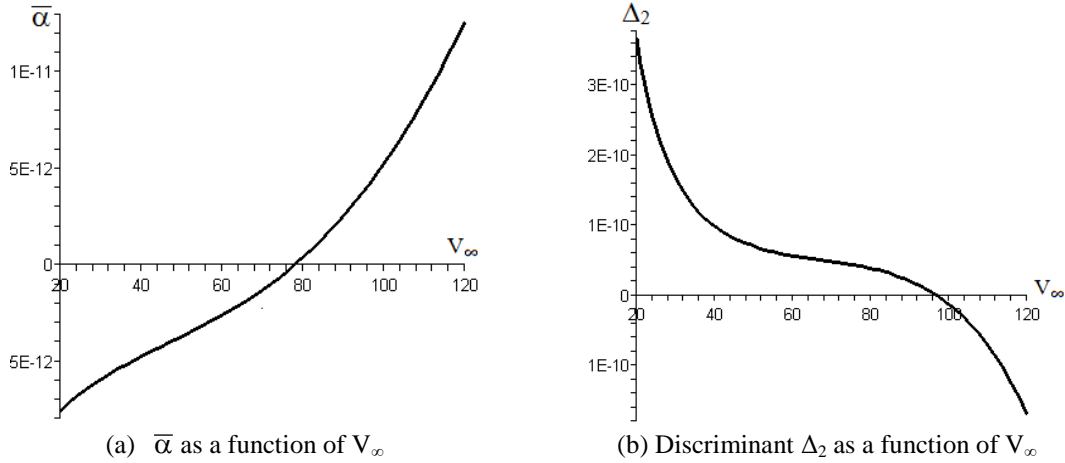


Fig. 9 The variables $\bar{\alpha}$ and Δ_2 for the Cessna 182

remain non-negative, it is necessary that t_f be limited so that $\tilde{W}(t_f)$ remains outside of $\bar{I}_{\tilde{W}}$, i.e.,

$$\tilde{W}(t_f) \geq \tilde{W}_{1+} \tag{23}$$

8.2 Sufficiency of power available

The airplane propelling system should be able to provide enough power for the motion to be possible. Thus, it is required that

$$P_R \leq P_{Amax} \tag{24}$$

We recall that the available power varies with altitude as follows

$$P_A(h) = P_A(0) \left[\frac{T(h)}{T_s} \right]^{4.2433} \tag{25}$$

Upon using Eqs. (17) and (25), Ineq. (24) can be written as

$$Q_1(\tilde{W}) \leq 0 \text{ with } Q_1(\tilde{W}) = \delta \tilde{W}^2 + \beta \tilde{W} + \left[\alpha - \frac{c P_{Amax}(0)}{\eta T_s^{4.2433}} \right] \tag{26}$$

The function Q_1 is identical to the function Q discussed in Section 8.1, except that its intercept on the ordinate axis is $\bar{\alpha}$ instead of α , with

$$\bar{\alpha} = \alpha - \frac{c P_{Amax}(0)}{\eta T_s^{4.2433}} \tag{27}$$

Consequently, its discriminant Δ_2 is identical to Δ_1 , except that the intercept is replaced by $\bar{\alpha}$. Fig. 9(a) shows how $\bar{\alpha}$ varies with V_∞ . If $\Delta_2 < 0$, Q_1 has no real roots, and is therefore always

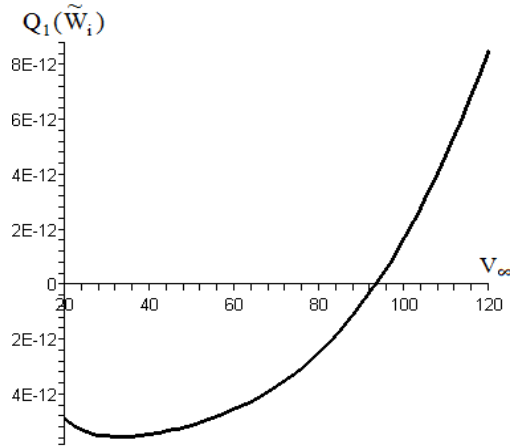


Fig. 10 $Q_1(\tilde{W}_i)$ as a function of V_∞ , when $R=800$ m and $\theta=-5^\circ$ for the Cessna 182

positive; Ineq. (24) is then never satisfied. It is therefore necessary that $\Delta_2 \geq 0$. This inequality imposes a restriction on the speed V_∞ . Fig. 9(b) shows how Δ_2 varies as a function of V_∞ , for the Cessna 182, when $\theta=-5^\circ$ and $R=800$ m.

We remark that the value of Δ_2 is independent of the sign of the inclination angle and of the weight W of the airplane. For the above mentioned trajectory, $\Delta_2 \geq 0$ only when $V_\infty < 96.9$ m/s. When $\Delta_2 \geq 0$, the two roots are

$$\tilde{W}_{2\pm} = \frac{1}{2\delta} [-\beta \pm \sqrt{\Delta_2}] \tag{28}$$

$\tilde{W}(t)$ must always remain in the interval $I_{\tilde{W}} = [\tilde{W}_{2-}, \tilde{W}_{2+}]$ for Ineq. (24) to hold. A necessary condition for this to be the case is certainly that it must hold at the initial time t_i , so that

$$Q_1(\tilde{W}_i) \leq 0 \tag{29}$$

This inequality imposes another constraint on the speed V_∞ . Fig. (10) shows how $Q_1(\tilde{W}_i)$ varies with the speed V_∞ , for the Cessna 182, when $R=800$ m and $\theta=-5^\circ$. In that case, Ineq. (29) is satisfied only when $V_\infty < 93.3$ m/s. Note that the fact that \tilde{W}_i satisfies Ineq. (26) means that it is in the interval $I_{\tilde{W}}$.

There now remains to ensure that Ineq. (26) is satisfied at all subsequent times. We shall distinguish the cases when the airplane is descending and when it is non-descending.

Case 1: The airplane is descending

β is then negative and the absolute minimum of $Q_1(\tilde{W})$ is on the positive \tilde{W} -axis. The following two different situations can occur.

1(a) $\bar{\alpha} \leq 0$: The root \tilde{W}_{2-} is then non-positive. The fact \tilde{W} is monotonically decreasing and positive, implies that $\tilde{W}_{2-} \leq \tilde{W}(t) \leq \tilde{W}_i \leq \tilde{W}_{2+}$ at all times and thus $Q_1(\tilde{W}) \leq 0$ at all times. No additional condition is then required.

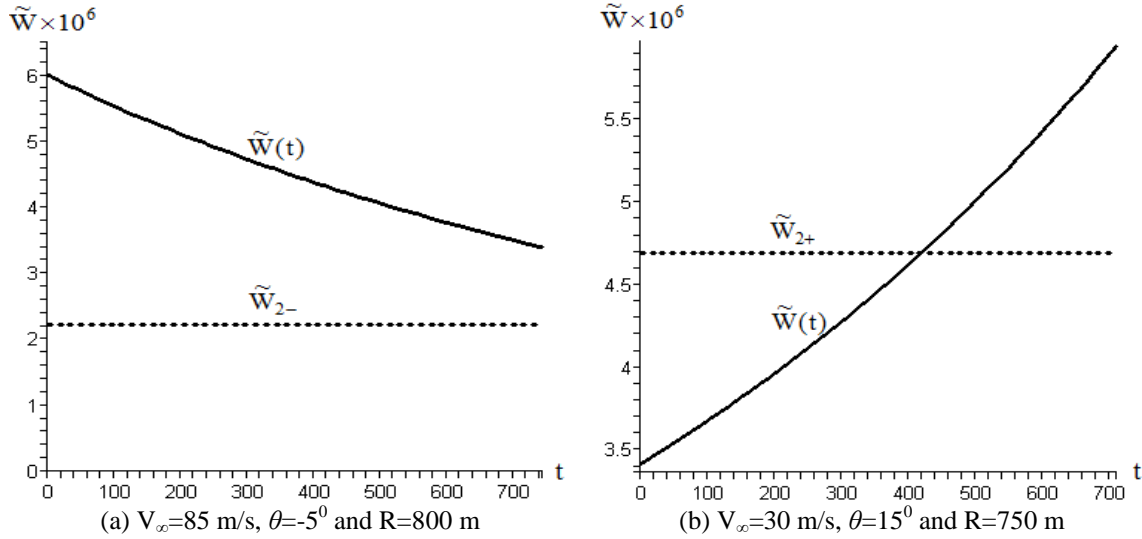


Fig. 11 $\tilde{W}(t)$ and its lower bound \tilde{W}_{2-} and its upper bound \tilde{W}_{2+} , for the Cessna 182

1(b) $\bar{\alpha} > 0$: The two roots \tilde{W}_{2-} and \tilde{W}_{2+} are positive. Ineq. (29) ensures that \tilde{W}_i is in the interval $I_{\tilde{W}}$ so that, since \tilde{W} is monotonically decreasing, it remains in the interval $I_{\tilde{W}}$ if t_f is limited such that

$$\tilde{W}_{2-} \leq \tilde{W}(t_f). \tag{30}$$

Fig. 11(a) shows how $\tilde{W}(t)$ changes in time with respect to \tilde{W}_{2-} , for the Cessna 182 with $\theta = -5^\circ$, $R = 800$ m, and $V_\infty = 85$ m/s. In that case, Ineq. (30) is satisfied for all times until the airplane reaches sea level.

Case 2: The airplane is non-descending

In that case, $\beta \geq 0$, and since the first two terms in Q_1 are positive, Ineq. (26) can only be satisfied if the third term of Q_1 is negative, that is if $\bar{\alpha} < 0$. This corresponds to a constraint on the values of V_∞ that is independent on the values of the radius R , the angle θ and the weight of the airplane W . Its value is a fixed characteristic of the airplane parameters, and it can therefore be calculated once for all. Fig. 9(a) shows how $\bar{\alpha}$ varies as a function of V_∞ , for the Cessna 182. In that case, one can determine that it is negative only when $V_\infty < 78.0$ m/s. When $\bar{\alpha} < 0$, the root \tilde{W}_{2-} of Q_1 will be negative while its other root \tilde{W}_{2+} is positive. $Q_1(\tilde{W}) \leq 0$ will then be true for all \tilde{W} if and only if

$$\tilde{W}(t) \leq \tilde{W}_{2+} \quad \forall t. \tag{31}$$

This inequality was ensured to hold at $t = t_i$; it will then determine the maximum value that t_f can have, as the first instant at which this inequality does not hold. Fig. 11(b) shows how $\tilde{W}(t)$ changes with time with respect to \tilde{W}_{2+} , for the Cessna 182 with $\theta = 15^\circ$, $R = 750$ m, and $V_\infty = 30$ m/s.

9. Flyability analysis for ascending flights

We have derived the conditions under which helical trajectories are flyable in terms of the airplane dynamical abilities. We cannot solve all of them together in order to obtain explicit range formulas for each parameter. Nevertheless, our results can be used to devise a procedure for testing whether trajectories are flyable or not. We describe this procedure below and show how it can be used to produce tables of parameters for flyable trajectories.

9.1 Procedure

1. Select an angle of inclination θ .
2. Compute the lower bound R_{LB} on R for which Ineq. (11), which guarantees that the bound on the lift coefficient, is respected. Select a value for R .
3. Compute the upper bound V_{UB1} on V_∞ according to Ineq. (7), which is required by the bound on the load factor.
4. Compute the lower bound V_{LB1} on V_∞ according to Ineq. (12), which guarantees that the bound on the lift coefficient, is respected
5. Calculate $\bar{\alpha}$ defined below Eq. (26), and determine the upper bound V_{UB2} on V_∞ for which $\bar{\alpha} < 0$.
6. Calculate the discriminant Δ_2 and determine the upper bound V_{UB3} on V_∞ for which $\Delta_2 \geq 0$.
7. Determine the upper bound V_{UB4} on V_∞ , for which $Q_1(\tilde{W}_1) \leq 0$.
8. Select V_∞ according the upper bounds V_{UB1} , V_{UB2} , V_{UB3} , V_{UB4} , and the lower bound V_{LB1} .
9. Compute t_{f1} , the time at which the airplane would arrive at sea level with $h(t_{f1})=0$.
10. Compute $W(t)$ and $\tilde{W}(t)$.
11. Calculate the roots \tilde{W}_{2+} , according to Eq. (28) and determine the instant of time t_{f2} at which the inequality $\tilde{W}(t) \leq \tilde{W}_{2+}$ ceases to hold.
12. Calculate t_{f3} , the time at which all the fuel would be burned, i.e., $W_i - W(t_{f3}) = W_f$. The longest time of flight t_f is the smallest of t_{f1} , t_{f2} , t_{f3} .

Once this is done, one can calculate the amount of fuel used, and the final altitude reached on the helix. A table of allowed trajectory parameters can be produced for a particular airplane by successively performing the above procedure with various values of θ and R . We will show an example of this procedure in the next section.

9.2 Construction of flyability tables

In order to illustrate the proposed method, we construct flyability tables for a few values of θ , these values increase discretely until the maximum possible inclination is reached. In all cases, the initial weight of the airplane is such that it carries half its maximum load, which includes a full tank of fuel. All ascending trajectories start at sea level so that $h(t_i)=0$.

The first line of the tables contains the value of θ , the minimum radius R_m and the minimum and maximum speeds V_m and V_M . The tables normally contain the trajectory parameters for the two speeds: these are V_m and V_M . However, a smaller value than V_M is used when the trajectory with V_M would last less than 3 seconds. For each selected speed, the parameters shown are: the maximum altitude that can be reached, the time and amount of fuel it takes to reach it. Although

Table 1 Cessna 182 trajectories ascending at 5°

| $\theta = 5^\circ$ | $R_m = 784$ m | $V_m = 28.2$ m/s | $V_M = 63.8$ m/s | |
|--------------------|---------------|------------------|------------------|----------|
| | h_f (m) | t_f (sec) | Fuel (N) | Fuel (%) |
| V_m | 5517 | 2245 | 145 | 8.3 |
| 63.0 | 500 | 91 | 11.4 | 0.7 |

Table 2 Cessna 182 trajectories ascending at 15°

| $\theta = 15^\circ$ | $R_m = 737$ m | $V_m = 27.7$ m/s | $V_M = 42.6$ m/s | |
|---------------------|---------------|------------------|------------------|----------|
| | h_f (m) | t_f (sec) | Fuel (N) | Fuel (%) |
| V_m | 3674 | 513 | 61 | 3.5 |
| 42.0 m/s | 195 | 18 | 2.6 | 0.15 |

Table 3 Cessna 182 trajectories ascending at 25°

| $\theta = 25^\circ$ | $R_m = 370$ m | $V_m = 20.3$ m/s | $V_M = 29.1$ m/s | |
|---------------------|---------------|------------------|------------------|----------|
| | h_f (m) | t_f (sec) | Fuel (N) | Fuel (%) |
| V_m | 2480 | 289 | 46 | 2.6 |
| 29.0 m/s | 56.4 | 4.6 | 0.8 | 0.05 |

Table 4 Silver Fox like UAV trajectories ascending at 5°

| $\theta = 5^\circ$ | $R_m = 233$ m | $V_m = 15.4$ m/s | $V_M = 41.5$ m/s | |
|--------------------|---------------|------------------|------------------|----------|
| | h_f (m) | t_f (sec) | Fuel (N) | Fuel (%) |
| V_m | 3700 | 2757 | 1.14 | 5.95 |
| 41.0 m/s | 122 | 34 | 0.04 | 0.20 |

Table 5 Silver Fox like UAV trajectories ascending at 25°

| $\theta = 25^\circ$ | $R_m = 193$ m | $V_m = 14.7$ m/s | $V_M = 25.0$ m/s | |
|---------------------|---------------|------------------|------------------|----------|
| | h_f (m) | t_f (sec) | Fuel (N) | Fuel (%) |
| V_m | 3700 | 596 | 0.73 | 3.81 |
| 24 m/s | 596 | 59 | 0.08 | 0.44 |

Table 6 Silver Fox like UAV trajectories ascending at 45°

| $\theta = 45^\circ$ | $R_m = 118$ m | $V_m = 13.0$ m/s | $V_M = 16.9$ m/s | |
|---------------------|---------------|------------------|------------------|----------|
| | h_f (m) | t_f (sec) | Fuel (N) | Fuel (%) |
| V_m | 2681 | 292 | 0.54 | 2.82 |
| 16.0 m/s | 615 | 54 | 0.10 | 0.55 |

we have not proved it explicitly, we expect that solutions exist for all radii larger than R_m , and all speeds between V_m and V_M .

9.2.1 Cessna 182

Tables 1-3 are constructed for the angles of climb $\theta=5^\circ$, 15° and 25° , which is the steepest angle

Table 7 C-130 Hercules trajectories ascending at 5^0

| $\theta = 5^0$ | $R_m = 3943$ m | $V_m = 63.1$ m/s | $V_M = 122.2$ m/s | |
|----------------|----------------|------------------|-------------------|----------|
| | h_f (m) | t_f (sec) | Fuel (N) | Fuel (%) |
| V_m | 5017 | 912 | 4153 | 1.56 |
| 118.0 m/s | 155 | 14.7 | 122 | 0.05 |

Table 8 C-130 Hercules trajectories ascending at 10^0

| $\theta = 10^0$ | $R_m = 3854$ m | $V_m = 62.8$ m/s | $V_M = 79.6$ m/s | |
|-----------------|----------------|------------------|------------------|----------|
| | h_f (m) | t_f (sec) | Fuel (N) | Fuel (%) |
| V_m | 1747 | 160 | 1114 | 0.42 |
| 62.0 m/s | 69 | 5 | 42 | 0.02 |

for which a helical trajectory can be flown.

9.2.2 Silver fox like UAV

Tables 4-6 are constructed for the angles of climb $\theta=5^0$, 25^0 and 45^0 , which is the steepest angle for which a helical trajectory can be flown.

9.2.3 C-130 hercules

Tables 7-8 are constructed for the angles of climb $\theta=5^0$ and 10^0 , which is the steepest angle for which a helical trajectory can be flown.

10. Flyability analysis for descending flights

Descending flights differ from ascending ones in that conditions have to be imposed to guarantee that the power required remains positive. Beside having to ensure the satisfaction of these additional constraints, the procedure is similar to that for ascending flights.

10.1 Procedure

1. Select an angle of inclination θ .
2. Compute the lower bound R_{LB} on R for which Ineq. (11), which guarantees that the bound on the lift coefficient, is respected. Select a value for R .
3. Compute the upper bound V_{UB1} on V_∞ according to Ineq. (7), which is required by the bound on the load factor.
4. Compute the lower bound V_{LB1} on V_∞ according to Ineq. (12), which guarantees that the bound on the lift coefficient, is respected
5. Calculate the discriminant Δ_0 , given in Eq. (20). If $\Delta_0 \leq 0$ then the power required is always non-negative; continue the procedure at Step 7 below.
6. If $\Delta_0 > 0$, calculate the forbidden interval $\bar{I}_V = (\sqrt{r_{0-}}, \sqrt{r_{0+}})$ for the speed V_∞ , according to Eq. (21). V_∞ has to be outside of this interval for P_R to be non-negative at the initial time t_i .
7. Determine the upper bound V_{UB2} on V_∞ for which $\Delta_2 \geq 0$.
8. Determine the upper bound V_{UB3} on V_∞ , for which $Q_1(\tilde{W}_i) \leq 0$.

Table 9 Cessna 182 trajectories descending at 5^0

| $\theta = -5^0$ | $R_m = 784$ m | $V_{m1} = 28.2$ m/s $V_{M1} = 41.1$ m/s | $V_{m2} = 78.0$ m/s $V_{M2} = 53.7$ m/s | |
|-----------------|---------------|--|--|----------|
| | h_f (m) | t_f (sec) | Fuel (N) | Fuel (%) |
| V_{m1} | 0 | 2245 | 18.2 | 1.0 |
| V_{M1} | 5499 | 5 | 0.0 | 0.0 |
| V_{m2} | 0 | 1179 | 3.8 | 0.2 |
| V_{M2} | 0 | 812 | 38.2 | 2.2 |

Table 10 Cessna 182 trajectories descending at 10^0

| $\theta = -10^0$ | $R_m = 766$ m | $V_m = 92.6$ m/s | $V_M = 112.1$ m/s | |
|------------------|---------------|------------------|-------------------|----------|
| | h_f (m) | t_f (sec) | Fuel (N) | Fuel (%) |
| V_m | 0 | 343 | 10.5 | 0.6 |
| 111 m/s | 5090 | 22 | 1.6 | 0.1 |

9. Select V_∞ according the upper bounds $V_{UB1}, V_{UB2}, V_{UB3}$, the lower bound V_{LB1} and, if $\Delta_0 > 0$, ensure that V_∞ is outside the forbidden interval \bar{I}_V .

10. Compute t_{f1} , the time at which the airplane would arrive at sea level with $h(t_{f1}) = 0$.

11. Compute $W(t)$ and $\tilde{W}(t)$.

12. If $\Delta_0 > 0$, the following steps are required.

- Calculate $\Delta_1 = \beta^2 - 4\alpha\delta$, the discriminant of Q. If $\Delta_1 > 0$ then Step 12 is finished.

- If $\Delta_1 \geq 0$, calculate the roots \tilde{W}_{1-} and \tilde{W}_{1+} , according to Eq. (2). If $\tilde{W}_i \leq \tilde{W}_{1-}$, then Step 12 is finished.

- $\tilde{W}_i \geq \tilde{W}_{1+}$, determine the last instant of time t_{f2} at which the inequality $\tilde{W}(t) \geq \tilde{W}_{1+}$ holds.

13. Calculate $\bar{\alpha}$: if $\bar{\alpha} \leq 0$, then no further steps are required. Continue to Step 16.

14. If $\bar{\alpha} > 0$, calculate the roots \tilde{W}_{2-} , according to Eq. (28). Determine the last instant of time t_{f3} at which the inequality $\tilde{W}_{2-} \leq \tilde{W}(t)$ holds.

15. Calculate t_{f4} , the time at which all the fuel would be burned, i.e., $W_i - W(t_{f4}) = W_f$.

16. The smallest of $t_{f1}, t_{f2}, t_{f3}, t_{f4}$ is the latest instant of time at which all the required conditions for the flyability of the trajectory are met.

Once this is done, one can calculate the amount of fuel used, and the final altitude reached on the helix. A table of allowed trajectory parameters can be produced for a particular airplane by successively performing the above procedure with various values of θ and R. We will show an example of this procedure in the next section.

10.2 Construction of flyability tables

Tables are constructed for a few values of θ , these values decrease until the maximum possible inclination is reached. In all cases, the initial weight of the airplane is such that it carries half its maximum load, comprising a full tank of fuel. All trajectories start at the service ceiling so that $h(t_i) = h_c$.

Table 11 Silver Fox like UAV trajectories descending at 5^0

| $\theta = -5^0$ | $R_m = 233$ m | $V_m = 27.6$ m/s | $V_M = 53.1$ m/s | |
|-----------------|---------------|------------------|------------------|----------|
| | h_f (m) | t_f (sec) | Fuel (N) | Fuel (%) |
| V_m | 0 | 1538 | 0.04 | 0.2 |
| V_M | 3576 | 27 | 0.02 | 0.1 |

Table 12 Silver Fox like UAV trajectories descending at 10^0

| $\theta = -10^0$ | $R_m = 228$ m | $V_m = 43.4$ m/s | $V_M = 60.0$ m/s | |
|------------------|---------------|------------------|------------------|----------|
| | h_f (m) | t_f (sec) | Fuel (N) | Fuel (%) |
| V_m | 0 | 491 | 0.05 | 0.3 |
| 59.0 m/s | 2797 | 88 | 0.10 | 0.5 |

Table 13 Silver Fox like UAV trajectories descending at 15^0

| $\theta = -15^0$ | $R_m = 219$ m | $V_m = 53.8$ m/s | $V_M = 65.0$ m/s | |
|------------------|---------------|------------------|------------------|----------|
| | h_f (m) | t_f (sec) | Fuel (N) | Fuel (%) |
| V_m | 0 | 266 | 0.06 | 0.3 |
| V_M | 3072 | 37 | 0.2 | 1.1 |

Table 14 C-130 Hercules trajectories descending at 2.5^0

| $\theta = -2.5^0$ | $R_m = 3966$ m | $V_m = 63.2$ m/s | $V_M = 217.1$ m/s | |
|-------------------|----------------|------------------|-------------------|----------|
| | h_f (m) | t_f (sec) | Fuel (N) | Fuel (%) |
| V_m | 0 | 2543 | 2454 | 0.9 |
| V_M | 6846 | 17.3 | 70.3 | 0.03 |

Table 15 C-130 Hercules trajectories descending at 5^0

| $\theta = -5^0$ | $R_m = 3943$ m | $V_{m1} = 63.1$ m/s $V_{M1} = 67.5$ m/s | $V_{m2} = 229.0$ m/s $V_{M2} = 268.6$ m/s | |
|-----------------|----------------|--|--|----------|
| | h_f (m) | t_f (sec) | Fuel (N) | Fuel (%) |
| V_{m1} | 5827 | 215 | 39.7 | 0.01 |
| 66.5 m/s | 6743 | 46 | 2.0 | 0.00 |
| V_{m2} | 0 | 351 | 870 | 0.3 |
| 267 m/s | 6659 | 15 | 59.8 | 0.02 |

The first line of the tables contains the value of θ , the minimum radius R_m , the minimum and maximum speeds V_m and V_M . When two ranges of speeds are possible, their respective lower limits will be denoted V_{m1} and V_{m2} and their upper limits V_{M1} and V_{M2} . Recall that this possibility of two separate domains of speeds was discussed in Section 8.1. All tables contain the trajectory parameters for only the speeds at the extremities of the possible ranges. A somewhat smaller speed than V_{M1} or V_{M2} is used when the trajectory with these speeds lasts less than 3 seconds. The content of the tables is the same as that in the tables for ascending trajectories. Again, we have not proved it explicitly, but we expect that solutions exist for all radii larger than R_m , and all speeds between the two extremities of speed ranges.

10.2.1 Cessna 182

Tables 9-10 are constructed for the angles of descent $\theta=-5^0$, and -10^0 , which is the steepest angle for which a helical trajectory can be flown.

10.2.2 Silver fox like UAV

Tables 11-13 are constructed for the angles of descent $\theta=-5^0$, -10^0 and -15^0 , which is the steepest angle for which a helical trajectory can be flown.

10.2.3 C-130 hercules

Tables 14-15 are constructed for the angles of descent, $\theta=-2.5^0$, and -5^0 , which is the steepest angle for which a helical trajectory can be flown.

11. Conclusions

We have obtained general formulas that express the necessary and sufficient conditions for an airplane to be able to follow an ascending or a descending helical trajectory. These formulas allow the determination of the possible angles of inclination of the trajectory, its minimum radius, the minimum and maximum speeds that the airplane can have on this trajectory, the fuel required, the time required to fly it, and the maximum and minimum altitude difference between the starting and the finishing points. We believe that these formulas are original in that no such results have been published before. They will find a definite usefulness in the construction of airplane trajectories that contain helical segments. They also constitute, in themselves, an important tool for the analysis of airplane performances.

In Section 9, we have demonstrated a procedure that allows for the production of tables of parameters for which ascending helical trajectories are possible. In Section 10, we have done the same for descending trajectories. We have presented sample applications of these procedures for three very different airplanes, namely the Cessna 182 Skylane, the Silver Fox UAV and the C-130 Hercules.

Here are some remarkable facts that are exhibited by the tables we have produced.

- In ascending trajectories, the maximum altitude reachable decreases as the angle of ascend increases and/or the speed increases. This is due to the fact that the power required to fly on these trajectories increases with these parameters, and thus the maximum power available is then reached earlier.

- When the airplane is ascending, its angle of inclination can be steeper than when it is descending. What limits the possibility of descending at constant speed is the force of gravity that tends to accelerate the fall of the airplane while it has no other mean of resisting the speed increase other than its drag.

- The range of possible values for V_∞ becomes narrower as the angle of inclination increases.

- The change in weight over the longest possible trajectory is rather small. For descending flights, in particular, it is always below 2.5% of the total amount of fuel. For ascending flights, it reaches up to 8.5% for the Cessna 182, 6% for the Silver Fox and 2% for the Hercules. As to be expected, the largest amount of fuel is required on trajectories with smaller inclination angles that are typically longer and last longer. Nevertheless, there would be many applications for which a reasonable approximation could consist in considering the weight of the airplane to be constant on the helical trajectory. This would certainly be valid in all cases, when only a short segment of the helical trajectory is flown. Such an approximation would entail a worthwhile simplification of the

computation requirements.

There are two important results presented in this article. The first one consists in new theoretical formulas that describe all dynamical aspects of an airplane flying on a helical trajectory. The second one is a method for constructing flyability tables for helical trajectories. Such tables would be very valuable in situations where it is not possible to perform, on-board the airplane, the calculations required for evaluating the mathematical expressions we derived. Once constructed, these tables could easily be stored in a memory on-board the airplane, from which the required parameters could be read when the need arises. This approach would clearly be appropriate for automatic trajectory planning even with small microcontrollers.

References

- Aeronautics Learning Laboratory for Science Technology and Research (ALLSTAR) of the Florida International University (2011), *Propeller Aircraft Performance and The Bootstrap Approach*.
- Airliners.net (2015), Santa Monica, California, U.S.A.
- Ambrosino, G., Ariola, M., Ciniglio, U., Corraro, F., De Lellis, E. and Pironti, A. (2009), "Path generation and tracking in 3-D for UAVs", *IEEE Trans. Contr. Syst. Technol.*, **17**(4), 980-988.
- Anderson, J.D. (2000), *Introduction to Flight*, 4th Edition, McGraw-Hill Series in Aeronautical and Aerospace Engineering, Toronto, Ontario, Canada.
- Babaei, A.R. and Mortazavi, M. (2010), "Three-dimensional curvature-constrained trajectory planning based on in-flight waypoints", *J. Aircr.*, **47**(4), 1391-1398.
- Beard, R.W. and McLain, T.W. (2015), *Implementing Dubins Airplane Paths on Fixed-Wing UAVs*, Handbook for Unmanned Aerial Vehicles, Springer Netherlands, Section XII, 1677-1701.
- Boukraa, D., Bestaoui, Y. and Azouz, N. (2006), "A new approach to trajectories planner design for a subsonic autonomous aerial fixed wing vehicle", *Proceedings of the 2006 American Control Conference*, Minneapolis, Minnesota, U.S.A., June.
- Cavcar, M. (2004), *Propeller*, Anadolu University, Eskisehir, Turkey.
- Chandler, P., Rasmussen, S. and Pachter, M. (2000), "UAV cooperative path planning", *Proceedings of the AIAA Guidance, Navigation, and Control Conference*, Denver, Colorado, U.S.A., August.
- Chitsaz, H. and LaValle, S.M. (2007), "Time-optimal paths for a dubins airplane", *Proceedings of the 46th IEEE Conference on Decision and Control*, New Orleans, Louisiana, U.S.A., December.
- Commercial Aviation Safety Team (CAST) (2011), *Propeller Operation and Malfunctions Basic Familiarization for Flight Crews*.
- Cowley, W.L. and Levy, H. (1920), *Aeronautics Theory and Experiment*, 2nd Edition, Edward Arnold, London, U.K.
- Crawford, D.J. and Bowles, R.L. (1975), *Automatic Guidance and Control of a Transport Aircraft During a Helical Landing Approach*, NASA technical note D-7980, NASA Langley Research Center, Hampton.
- Dai, R. and Cochran, J.E. (2009), "Three-dimensional trajectory optimization in constrained airspace", *J. Aircr.*, **46**(2), 627-634.
- Dubins, L.E. (1957), "On curves of minimal length with a constraint on average curvature and with prescribed initial and terminal positions and tangents", *Am. J. Math.*, **79**(3), 497-516.
- Etkin, B. (1972), *Dynamics of Atmospheric Flight*, John Wiley and Sons, Inc., New York, U.S.A.
- Filippone, A. (2000), "Data and performances of selected aircraft and rotorcraft", *Prog. Aerosp. Sci.*, **36**(8), 629-654.
- Frazzoli, M., Dahleh, A. and Feron, E. (2005), "Maneuver-based motion planning for nonlinear systems with symmetries", *IEEE Trans. Robot.*, **21**(6), 1077-1091.
- Granelli, F. (2007), *Carl Goldberg Falcon 56*, The Academy of Model Aeronautics' Sport Aviator, the E-Zine for the Newer RC Pilot.
- Hota, S. and Ghose, D. (2010), "Optimal geometrical path in 3D with curvature constraint", *Proceedings of*

- the *IEEE/RSJ International Conference on Intelligent Robots and Systems (IROS)*, Taipei, Taiwan, October.
- Hwangbo, M., Kuffner, J. and Kanade, T. (2007), "Efficient two-phase 3D motion planning for small fixed-wing UAVs", *Proceedings of the IEEE International Conference on Robotics and Automation*, Rome, Italy, April.
- Jia, D. and Vagners, J. (2004), "Parallel evolutionary algorithms for UAV path planning", *Proceedings of the AIAA 1st Intelligent Systems Technical Conference*, Chicago, Illinois, U.S.A., September.
- Kamm, R.W. (2002), "Mixed up about fuel mixtures", *Aircraft Maintenance Technology*.
- Labonté, G. (2012), "Formulas for the fuel of climbing propeller driven planes", *Aircr. Eng. Aerosp. Technol.*, **84**(1), 23-36.
- Labonté, G. (2015), "Simple formulas for the fuel of climbing propeller driven airplanes", *Adv. Aircraft Spacecraft Sci.*, **2**(4), 367-389.
- Labonté, G. (2016), "Airplanes at constant speeds on inclined circular trajectories", *Adv. Aircraft Spacecraft Sci.*, **3**(4), 399-425.
- Li, X., Xie, J., Cai, M., Xie, M. and Wang, Z. (2009), "Path planning for UAV based on improved A* algorithm", *Proceedings of the 9th International Conference on Electronic Measurement & Instruments*, Beijing, China, August.
- Lockheed Martin (2013), *C-130J Super Hercules, Whatever the Situation, We'll be There*.
- Mair, W.A. and Birdsall, D.L. (1992), *Aircraft Performance*, Cambridge Aerospace Series 5, Cambridge University Press, Cambridge, U.K.
- McIver, J. (2003), *Cessna Skyhawk II/100*, Performance Assessment, Temporal Images, Melbourne, Australia.
- Narayan, P.P., Wu, P.P. and Campbell, D.A. (2008), "Unmanning UAVs-addressing challenges in on-board planning and decision making", *Proceedings of the 1st International Conference on Humans Operating Unmanned Systems*, Brest, France, September.
- Phillips, W.F. (2004), *Mechanics of Flight*, John Wiley & Sons, Inc., Hoboken, New Jersey, U.S.A.
- Roud, O. and Bruckert, D. (2006), *Cessna 182 Training Manual*, Red Sky Ventures and Memel CATS, 2nd Edition 2011, Windhoek, Namibia.
- Sadraey, M.H. (2013), *Aircraft Design: A Systems Engineering Approach*, Aerospace Series, John Wiley & Sons Ltd, Toronto, Ontario, Canada.
- Stewart Air Force Base Reunion (2005), *C-130 Hercules Specifications*.
- Sussmann, H.J. (1995), "Shortest 3-dimensional paths with a prescribed curvature bound", *Proceedings of the 34th IEEE Conference on Decision and Control*, New Orleans, U.S.A., December.
- Tsiotras, P., Bakolas, E. and Zhao, Y. (2011), "Initial guess generation for aircraft landing trajectory optimization", *Proceedings of the AIAA Guidance, Navigation, and Control Conference*, Portland Oregon, U.S.A., August.
- UAVGLOBAL Unmanned Systems and Manufacturers (2016), *BAE Systems Silver Fox*.
- Von Mises, R. (1945), *Theory of Flight*, Dover Publications Inc., New York, U.S.A.

Appendix A: Reference airplanes

We note that there could be small differences between the values we list here and the actual values for a particular model of these airplanes. We used values that were available on the internet or were estimated from the values for similar airplanes. These data are quite adequate for our purpose that is to illustrate the calculations involved in the formulas we have derived.

The thrust of the Cessna 182 and that of the C-130 Hercules is provided by a reciprocating engine with constant speed propeller; that of the Silver Fox by a reciprocating engine with a fixed pitch propeller. We recall that the efficiency of the propeller is a function of the advance ratio J , defined as

$$J = \frac{V_{\infty}}{ND}$$

in which N is its number of revolution per second and D is its diameter. Thus the maximum power available P_{Amax} will depend on the speed, according to the equation

$$P_{Amax} = \eta(J)P_{max}$$

The dependence of η on J for a constant speed propeller has the general features shown in Fig. 12(a). This curve approximates that given in Cavcar (2004) by the following quadratic expressions

$$\eta(J) = \begin{cases} \left[\frac{0.663}{0.640} \right] [J - 0.8]^2 + 0.8 & \forall J \leq 0.8 \\ \eta(J) = 0.8 & \forall J > 0.8 \end{cases}$$

The dependence of η on J for a fixed pitch propeller has the general features shown in Fig. 12(b). This curve approximates that given in the Aeronautics Learning Laboratory for Science Technology and Research (ALLSTAR) of the Florida International University (2011) by the following quadratic expressions

$$\eta(J) = \begin{cases} -\left[\frac{0.83}{0.49} \right] [J - 0.70]^2 + 0.83 & \forall J \leq 0.7 \\ -\left[\frac{0.83}{0.06} \right] [J - 0.70]^2 + 0.83 & \forall J > 0.7 \end{cases}$$

Note that the propeller efficiency of this fixed pitch propellers goes to 0 at $V_{\infty}=66.1$ m/s and becomes negative after that. Although a negative propeller efficiency might be desirable to slow down the airplane when it descends, it is not recommended to let this happens. When this happens, the propeller drives the engine and damage to the engine may result (see for example the Commercial Aviation Safety Team document 2011). We shall therefore not allow speeds larger than that value.

A.1 Cessna 182 skylane

The parameters listed are W_1 =the weight of the empty airplane, W_0 =the maximum take-off weight, W_F =the maximum weight of fuel, b =the wingspan, S =the wing area, e =Oswald's efficiency factor, C_{Lmax} =the maximum global lift coefficient, C_{D0} =the global drag coefficient at zero lift, n_{max} and n_{min} are respectively the maximum and minimum value of the load factor,

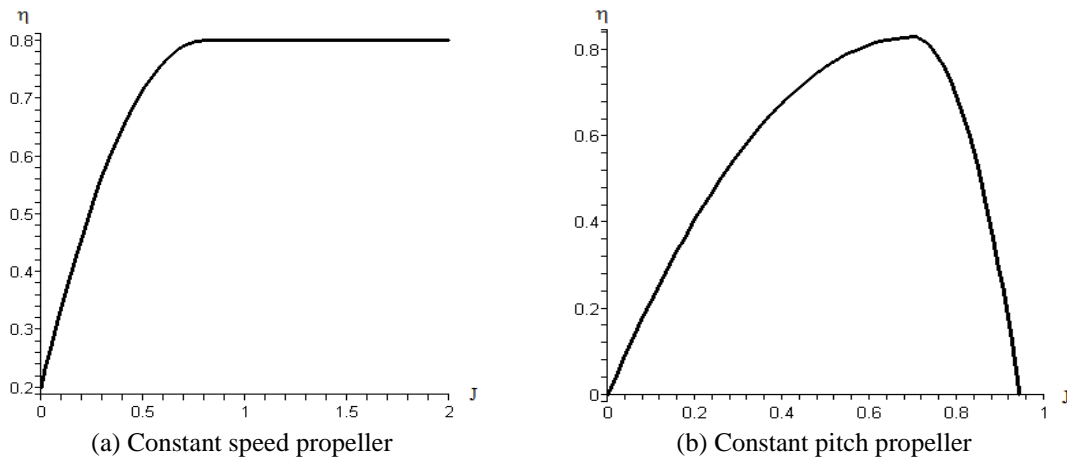


Fig. 12 Typical efficiency factor as a function of the advance ratio J

Table 16 Characteristic parameters of the cessna 182

| | | |
|---------------------------------|---------------------------|----------------------------------|
| $W_1 = 7,562 \text{ N}$ | $W_0 = 11,121 \text{ N}$ | $W_F = 1737 \text{ N}$ |
| $b = 11.02 \text{ m}$ | $S = 16.1653 \text{ m}^2$ | $e = 0.75$ |
| $C_{Lmax} = 2.10$ | $C_{D0} = 0.029$ | $n_{max} = 3.8, n_{min} = -1.52$ |
| $V_{NE} = 90 \text{ m/s}$ | $h_c = 5517 \text{ m}$ | |
| $P_{Amax} = 171.511 \text{ kW}$ | $RPM = 2,600$ | $c = 7.4475 \times 10^{-7}$ |
| Const. speed propeller | Diameter = 2.08 m | $\eta_{max} = 0.80$ |

Table 17 Characteristic parameters of the silver fox-like airplane

| | | |
|-------------------------------|-------------------------|---------------------------------|
| $W_1 = 72.35 \text{ N}$ | $W_0 = 119.6 \text{ N}$ | $W_F = 19.1 \text{ N}$ |
| $b = 2.4 \text{ m}$ | $S = 0.768 \text{ m}^2$ | $e = 0.8$ |
| $C_{Lmax} = 1.26$ | $C_{D0} = 0.0251$ | $n_{max} = 5.0, n_{min} = -2.0$ |
| $V_{NE} = 56.4 \text{ m/s}$ | $h_c = 3700 \text{ m}$ | |
| $P_{Amax} = 1.491 \text{ kW}$ | $RPM = 7,500$ | $c = 7.4475 \times 10^{-7}$ |
| Fixed pitch propeller | Diameter = 0.56 m | $\eta_{max} = 0.83$ |

V_{NE} =maximum speed allowed, h_c =the service ceiling, P_{Amax} =maximum breaking power at sea level, RPM =number of revolution per minute, c =the specific fuel consumption, Diameter=diameter of the propeller, η_{max} =maximum value of the propeller efficiency.

The characteristic parameters for the Cessna 182 can be found in Airlines.net (2015), Roud and Bruckert (2006) and McIver (2003). Some of the parameters, which were not readily available, were estimated from those of the very similar Cessna 172.

A.2 Silver fox like UAV

The Silver Fox UAV is presently produced by Raytheon. Some specifications for the Silver Fox can be found at UAVGLOBAL Unmanned Systems and Manufacturers (2016). The power available $P_A(0)$ for the Silver Fox is only about 370 W, which allows it to climb only at low

Table 18 Characteristic parameters of the C-130 hercules

| | | |
|------------------------------------|-------------------------------|-----------------------------------|
| $W_1 = 337,120 \text{ N}$ | $W_0 = 689,009 \text{ N}$ | $W_F = 266,717 \text{ N}$ |
| $b = 40.4 \text{ m}$ | $S = 162.1 \text{ m}^2$ | $e = 0.92$ |
| $C_{L_{\max}} = 2.7 \text{ (2)}$ | $C_{D0} = 0.0138 \text{ (1)}$ | $n_{\max} = 3.0, n_{\min} = -1.0$ |
| $V_{NE} = 186.4 \text{ m/s}$ | $h_c = 7010 \text{ m}$ | |
| $P_{A_{\max}} = 11,113 \text{ kW}$ | $\text{RPM} = 1020$ | $c = 7.4475 \times 10^{-7}$ |
| Const. speed propeller propeller | Diameter = 4.11 m | $\eta_{\max} = 0.81$ |

angles. Meanwhile, it is common for Radio Controlled (RC) airplanes to climb at very steep angles (See for example Granelli (2007)). Thus, upon taking advantage of motors that have been developed in this domain, a Silver Fox-like airplane could be endowed with much more power in order to improve considerably its manoeuvre envelope. One such motor is the O.S. 120AX 20cc that outputs 3.1 hp, i.e., 2312 W, and weights only 650 g; so we shall consider a Silver Fox-like UAV with this particular motor.

A.3 Lockheed C-130 Hercules

Some of its specifications are those of the Hercules itself, as can be found in Lockheed Martin (2013), Stewart Air Force Base (2005) and Sadraey (2013) and some parameters have been set at plausible values, by comparison with other available transport airplanes Filippone (2000).

Nomenclature

| | |
|------------------|---|
| a | speed of sound in air. At altitude h, $a(h) = \sqrt{\gamma R T(h)}$. At sea level, $a(0) = 340.3029$ m/s |
| a_1 | absolute value of the slope of the temperature as a function of altitude, below 11 km, $a_1 = 6.5 \times 10^{-3}$ K/m |
| AFR | air fuel ratio (about 14.7) |
| AR | aspect ratio = b^2/S |
| b | wingspan |
| c | specific fuel consumption in Newton per Watt-second, that is in m^{-1} |
| C_D | global drag coefficient for the aircraft = $C_{D0} + \frac{C_L^2}{\pi e AR}$ (Drag polar) |
| C_{D0} | global drag coefficient at zero lift |
| C_L | global lift coefficient for the aircraft |
| D | drag = $\frac{1}{2} \rho_\infty S C_D V_\infty^2$ |
| e | Oswald's efficiency factor |
| g | gravitational constant = 9.8 m/s ² |
| h | altitude of airplane |
| h_c | service ceiling |
| L | lift = $\frac{1}{2} \rho_\infty S C_L V_\infty^2$ |
| P | power of the engine in Watt |
| R | specific gas constant for air = 287.058 J/(kg K) |
| S | wing area |
| t | time variable |
| T_s | temperature at sea level = 288.16 K |
| $T(h)$ | temperature at altitude h |
| v_3 | vertical component of airplane velocity |
| V_∞ | airplane speed with respect to the undisturbed air in front of it |
| V_{NE} | speed never to be exceeded |
| W | weight of the airplane |
| W_1 | weight of the empty airplane |
| W_f | maximum weight of fuel |
| W_0 | maximum take-off weight (MTOW) |
| γ | ratio of the constant pressure specific heat to the constant volume specific heat = $c_p/c_v = 1.4$ for air |
| η | propeller efficiency |
| ρ_s | air density at sea level = 1.225 kg/m ³ |
| $\rho_\infty(h)$ | density of undisturbed air in front of airplane, at altitude h, $\rho_s \left[\frac{T(h)}{T_s} \right]^{4.2433}$ |